

# Constraint-induced movement therapy enhances AMPA receptor-dependent synaptic plasticity in the ipsilateral hemisphere following ischemic stroke

<https://doi.org/10.4103/1673-5374.290900>

Received: February 29, 2020

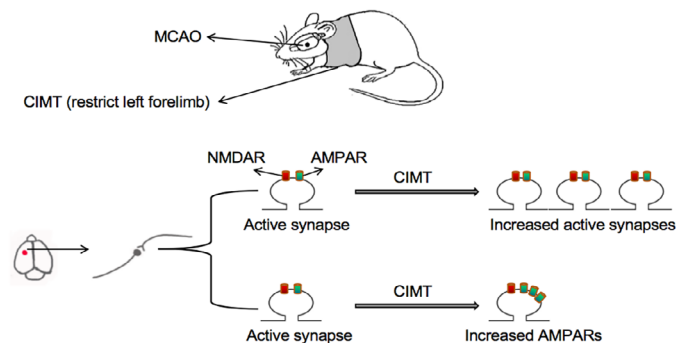
Peer review started: March 3, 2020

Accepted: April 7, 2020

Published online: August 24, 2020

Jian Hu<sup>#</sup>, Pei-Le Liu<sup>#</sup>, Yan Hua<sup>#</sup>, Bei-Yao Gao, Yu-Yuan Wang, Yu-Long Bai<sup>\*</sup>, Chan Chen<sup>\*</sup>

**Graphical Abstract** Constraint-induced movement therapy (CIMT) improves the functional recovery following stroke possibly through strengthening  $\alpha$ -amino-3-hydroxy-5-methyl-4-isoxazole propionic acid receptors (AMPA)-mediating synaptic transmission



## Abstract

Constraint-induced movement therapy (CIMT) can promote the recovery of motor function in injured upper limbs following stroke, which may be associated with upregulation of  $\alpha$ -amino-3-hydroxy-5-methyl-4-isoxazole propionic acid receptor (AMPA) at synapses in the ipsilateral sensorimotor cortex in our previous study. However, AMPAR distribution is tightly regulated, and only AMPARs on the postsynaptic membrane can mediate synaptic transmission. We speculated that synaptic remodeling induced by movement-associated synaptic activity can promote functional recovery from stroke. To test this hypothesis, we compared AMPAR expression on the postsynaptic membrane surface in a rat model of ischemic stroke induced by middle cerebral artery occlusion (MCAO) with *versus* without CIMT, which consisted of daily running wheel training for 2 weeks starting on day 7 after MCAO. The results showed that CIMT increased the number of glutamate receptor (GluR)2-containing functional synapses in the ipsilateral sensorimotor cortex, and reduced non-GluR2 AMPARs in the ipsilateral sensorimotor cortex and hippocampal CA3 region. In addition, CIMT enhanced AMPAR expression on the surface of post-synaptic membrane in the ipsilateral sensorimotor cortex and hippocampus. Thus, CIMT promotes the recovery of motor function of injured upper limbs following stroke by enhancing AMPAR-mediated synaptic transmission in the ischemic hemisphere. These findings provide supporting evidence for the clinical value of CIMT for restoring limb movement in stroke patients. All experimental procedures and protocols were approved by the Department of Laboratory Animal Science of Fudan University, China (approval No. 201802173S) on March 3, 2018.

**Key Words:** brain; experiment; injury; plasticity; regeneration; repair; stroke; synapse

Chinese Library Classification No. R455; R338.1+3; R741

## Introduction

Ischemic stroke is a leading cause of death and disability worldwide and constitutes a social and economic burden, with survivors often experiencing persistent sensorimotor and cognitive dysfunction (Writing Group Members et al., 2016; Benjamin et al., 2018). Rehabilitation training is the first-line intervention after ischemic stroke (Askim et al., 2009, 2010; Arya et al., 2011). Neural plasticity is critical for post-stroke recovery and rehabilitation (Wang et al., 2010; Carmichael, 2012; Alia et al., 2017); its efficacy has been linked to structural and functional reorganization in the damaged brain area, but also in the contralateral hemisphere (Bueteffisch, 2015; Jones and Adkins, 2015). Ischemic stroke can lead to

synaptic dysfunction (Li et al., 2013; Hofmeijer et al., 2014; Park et al., 2015); the focus of post-stroke rehabilitation is to restore plasticity to the residual synapses (Nie and Yang, 2017; Xie et al., 2019).

Glutamate is the main excitatory neurotransmitter in the central nervous system (CNS).  $\alpha$ -Amino-3-hydroxy-5-methyl-4-isoxazole propionic acid receptor (AMPA) and N-methyl-D-aspartic acid receptor (NR) are the main ionotropic glutamate receptors (GluRs) in the mammalian CNS; the former mediates most rapid excitatory synaptic transmission, and its regulation is critical for synaptic strength and efficacy (Carroll et al., 2001; Anggono and Huganir, 2012; Huganir and Nicoll, 2013). AMPARs in cortical and hippocampal pyramidal neurons are

Department of Rehabilitation Medicine, Huashan Hospital, Fudan University, Shanghai, China

**\*Correspondence to:** Yu-Long Bai, dr\_baiyl@fudan.edu.cn; Chan Chen, chanchen09@fudan.edu.cn. #These authors contributed equally to this study. <https://orcid.org/0000-0003-0461-1506> (Yu-Long Bai); <https://orcid.org/0000-0001-7629-2028> (Chan Chen)

**Funding:** This study was supported by the National Natural Science Foundation of China, Nos. 81871841 (to YLB) and 81601960 (to CC).

**How to cite this article:** Hu J, Liu PL, Hua Y, Gao BY, Wang YY, Bai YL, Chen C (2021) Constraint-induced movement therapy enhances AMPA receptor-dependent synaptic plasticity in the ipsilateral hemisphere following ischemic stroke. *Neural Regen Res* 16(2):319-324.

## Research Article

mainly composed of GluR1/2 and GluR2/3 heteromers (Geiger et al., 1995; Wenthold et al., 1996; Lu et al., 2009). Most AMPARs in the CNS are thought to contain a GluR2 subunit (Greger et al., 2002), which determines the major biophysical properties of the receptors given its impermeability to calcium (Cull-Candy et al., 2006; Shimshek et al., 2006; Isaac et al., 2007). Reduction of GluR2 and upregulation of Ca<sup>2+</sup>-permeable AMPARs, which lack GluR2 but contain GluR1 or GluR3, was found to be associated with increased vulnerability of neurons to excitotoxicity in cerebral ischemia, which is known as the GluR2 hypothesis (Dixon et al., 2009; Wang et al., 2011, 2012; Zhai et al., 2013). Synaptic plasticity depends on changes in AMPAR number and composition (Malinow and Malenka, 2002). We speculated that such synaptic remodeling induced by movement-associated synaptic activity is the mechanism underlying recovery from stroke. To test this hypothesis, in this study, we investigated the effect of constraint-induced movement therapy (CIMT) on the expression of postsynaptic AMPARs in the sensorimotor cortex and hippocampus in a rat model of ischemic stroke.

## Materials and Methods

### Animals

Specific-pathogen-free adult male Sprague-Dawley rats ( $n = 36$ ) weighing 260–280 g and aged 7–9 weeks were purchased from Shanghai SIPPR-BK LAB Animal Ltd. (Shanghai, China; license No. SCXK [Hu] 2018-0006). The rats were housed in cages at room temperature ( $23 \pm 1^\circ\text{C}$ ) and exposed to light for 12 hours a day, with free access to food and water. The rats were randomly and equally divided into three groups: CIMT (middle cerebral artery occlusion [MCAO] surgery with CIMT), MCAO (MCAO surgery without CIMT), and sham (sham surgery) (Figure 1A). For immunofluorescence and western blot analyses, there were six rats per group. Experimental procedures conformed to the animal ethics standards of the Department of Laboratory Animal Science of Fudan University, China (approval No. 201802173S) on March 3, 2018.

### MCAO model establishment

The MCAO model was established as previously described (Hu et al., 2019). Briefly, rats were anesthetized by intraperitoneal injection of 10% chloral hydrate (0.36 mL/100 g). A thread (Beijing Xinong Technology Co., Beijing, China; product No. 2636-A5) with silicone covering 5–6 mm of the front head was inserted into the left middle cerebral artery of the rat. The thread had a length of 45 mm and a diameter of 0.26 mm, with a head diameter of  $0.36 \pm 0.02$  mm. Ischemia time was 90 minutes. To ensure that the middle cerebral artery was blocked, the suture was inserted into the internal carotid artery at a depth of 18–20 mm. Rats in the sham group underwent the same procedure, except that there was no occlusion of the middle cerebral artery. The rats' body temperature was maintained at  $37^\circ\text{C}$  using a heating pad.

### CIMT

CIMT was initiated on day 7 after the surgery. The forelimb on the healthy (left) side of the rat was fixed with plaster lined on the inside with cotton pads to prevent direct contact between the plaster and skin. Rats in the CIMT group were forced to use their impaired forelimbs for daily activities such as eating and drinking, and 20 minutes of running wheel training was added every day for 2 weeks. The running wheel had a diameter of 35 cm, width of 9.5 cm, and spoke interval of 1.5 cm. Before behavioral assessment, the plaster was removed, and the restrained limbs were massaged and passively exercised to restore motor ability. Rats in the sham and MCAO groups were allowed to move freely in their cage without CIMT intervention.

### Foot-fault test

The foot-fault test was performed at 7, 14, and 21 days after surgery as previously described (Hua et al., 2019). The

equipment for the foot-fault test was composed of transparent Plexiglass and metal bars, and was designed and fabricated by our group according to the requirements of the test. The distance between metal bars was 2 cm and there were 34 bars at 30 cm above the ground, with the home cage placed at the end of the running ladder. The test was performed in a quiet environment. Each rat walked along the ladder three times during each test, with a camera recording the entire process. The total number of steps and number of empty steps on the affected side of the rats were used to calculate the foot fault ratio. The results of three trials were averaged.

### Immunofluorescence labeling

We used antibodies against the extracellular epitopes of NR1, GluR1, and GluR2 proteins to quantify surface expression and colocalization of these receptors by confocal imaging. Immunofluorescence labeling and analysis were performed as previously described (Mokin and Keifer, 2006; Zhou et al., 2011). Briefly, on day 21 after MCAO surgery, rats were anesthetized with 10% chloral hydrate and transcardially perfused with phosphate-buffered saline (PBS) and 4% paraformaldehyde. The brain was removed and fixed overnight in 4% paraformaldehyde. After dehydration in a gradient of 10%, 20%, and 30% sucrose solution at  $4^\circ\text{C}$ , the brain was frozen and cut into sections at a thickness of 20  $\mu\text{m}$  on a freezing microtome. The sections were washed three times with PBS, and antigen retrieval was performed by microwave irradiation; after three washes with PBS, the samples were blocked in PBS containing 10% goat serum for 1 hour at room temperature, and incubated overnight at  $4^\circ\text{C}$  with rabbit anti-NR1 antibody (1:100; Abcam, Cambridge, UK; Cat# 17345). After washing three times with PBS, the sections were incubated for 1 hour at room temperature with Cy3-conjugated goat anti-rabbit IgG (H+L) (1:300; Servicebio, Wuhan, Hubei Province, China; Cat# GB21303). The sections were washed with PBS, then incubated overnight at  $4^\circ\text{C}$  with mouse anti-GluR1 (1:100; Abcam; Cat# ab174785) or mouse anti-GluR2 (1:100; Merck KGaA, Darmstadt, Germany; Cat# MAB397) antibody, followed by Alexa Fluor 488-conjugated Affinipure goat anti-mouse IgG (H+L) (1:400; Servicebio; Cat# GB25301) for 1 hour at room temperature. After washing three times with PBS, nuclei were stained with DAPI at room temperature for 10 minutes, and the sections were washed with PBS and mounted. Images were acquired with a confocal microscope (LSM510; Zeiss, Jena, Germany) using a 63 $\times$  oil-immersion objective, and were processed and analyzed using ImageJ software (National Institutes of Health, Bethesda, MD, USA). The signal threshold was at least twice the background intensity, and areas outside the cell body were selected for colocalization analysis. Mander's overlap coefficient (with values ranging from 0 to 1) was used as an index to evaluate the degree of colocalization.

### Synaptosome preparation

Syn-PER synaptic protein extraction reagent (Thermo Fisher Scientific, Waltham, MA, USA; Cat# 87793) was used to prepare synaptosomes. Rats were anesthetized and sacrificed 21 days after surgery. The ipsilateral sensorimotor cortex and hippocampus were rapidly removed and weighed, and ten volumes (1 g:10 mL) of Syn-PER reagent containing protease and phosphatase inhibitors was added. The tissue was ground at 50 r/s for 5 minutes; the homogenate was centrifuged at  $4^\circ\text{C}$  and  $1200 \times g$  for 10 minutes, and the supernatant was centrifuged at  $4^\circ\text{C}$  and  $15,000 \times g$  for 20 minutes. The resultant pellet (synaptosome fraction) was resuspended in Syn-PER reagent, and protein concentration was measured with the bicinchoninic acid method (Beyotime, Haimen, China; Cat# P0012).

### Surface biotinylation of GluR1 and GluR2 in synaptosomes

Synaptosome preparations (500  $\mu\text{g}$  of protein/tube) were incubated with PBS/Ca<sup>2+</sup>/Mg<sup>2+</sup> buffer containing 0.5 mg/mL EZ-Link Sulfo-NHS-SS-Biotin (Thermo Fisher Scientific; Cat#

21945) for 1 hour at 4°C with gentle shaking. Glycine-containing PBS/Ca<sup>2+</sup>/Mg<sup>2+</sup> buffer (100 mM; 1 mL) was then added and incubated on ice for 10 minutes to terminate the biotinylation reaction, and the sample was then centrifuged at 4°C and 8000 × *g* for 4 minutes. The supernatant was discarded, and the pellet was resuspended in 1 mL of glycine-containing PBS/Ca<sup>2+</sup>/Mg<sup>2+</sup> buffer (100 mM) followed by centrifugation at 4°C and 8000 × *g* for 4 minutes. This step was repeated, and the pellet was resuspended in 1 mL of 100 mM glycine-containing PBS/Ca<sup>2+</sup>/Mg<sup>2+</sup> buffer, followed by incubation at 4°C for 30 minutes with gentle shaking and centrifugation at 4°C and 8000 × *g* for 4 minutes. The pellet was resuspended in 1 mL of PBS/Ca<sup>2+</sup>/Mg<sup>2+</sup> buffer and centrifuged at 4°C and 8000 × *g* for 4 minutes. This step was repeated 2 more times, and the final pellet was incubated in 250 μL of 1% Triton X-100 buffer containing protease inhibitor at 4°C for 30 minutes with shaking, then centrifuged at 4°C and 20,000 × *g* for 30 minutes. One-third of the supernatant was taken as the total synaptosome fraction. The remaining supernatant was mixed with 200 μL NeutrAvidin agarose resin (Thermo Fisher Scientific; Cat# 29200) and incubated overnight at 4°C with gentle shaking. The samples were centrifuged at 4°C and 17,700 × *g* for 4 minutes. The biotinylated protein/avidin pellets were resuspended in 1 mL of 1% Triton X-100 buffer and centrifuged at 4°C and 17,700 × *g* for 4 minutes. This step was repeated 2 more times, and 100 μL Laemmli buffer (Beyotime; Cat# P0015) was added; the mixture was incubated at room temperature for 20 minutes with gentle shaking to elute the biotinylated protein. The samples were centrifuged at 4°C and 17,700 × *g* for 4 minutes and the supernatant containing the biotinylated synaptic membrane surface protein was collected. Total samples were prepared for western blot analysis by adding sample loading buffer. Both total and biotinylated samples were heated at 95°C for 5 minutes and stored at -20°C.

### Western blot analysis

Total and biotinylated protein samples were electrophoretically separated on 7.5% polyacrylamide gels. The proteins were transferred to a polyvinylidene difluoride membrane (Merck KGaA; Cat# IPVH00010). After blocking with 3% bovine serum albumin for 1 hour, the membrane was incubated overnight at 4°C with the following primary antibodies: rabbit anti-GluR2 (1:1000; Abcam; Cat# ab20673), mouse anti-GluR1 (1:1000; Abcam; Cat# ab174785), and rabbit anti-tubulin (1:3000; Abways, Shanghai, China; Cat# AB0049). The secondary antibodies were peroxidase-conjugated goat anti-rabbit and goat anti-mouse IgG (H+L) (1:5000; Jackson ImmunoResearch Laboratories, West Grove, PA, USA; Cat# 124791 and 127655, respectively). Protein bands were detected using an ultrasensitive chemiluminescence kit (Beyotime; Cat# P00185) and FluorChem Q imager (Alpha Innotech, San Leandro, CA, USA). The gray value was analyzed using ImageJ software. Total GluR1 and GluR2 levels were normalized to tubulin levels. Surface expression of GluR1 and GluR2 was calculated by determining the relative ratios of biotinylated GluR1 and GluR2 to total GluR1 and GluR2, respectively.

### Statistical analysis

Data were analyzed using Prism v7 software (GraphPad, La Jolla, CA, USA). Differences in behavioral data were evaluated by two-way analysis of variance with Tukey's multiple comparisons test; and data from immunofluorescence labeling and western blotting experiments were evaluated by one-way analysis of variance and Tukey's multiple comparisons test. Data are presented as the mean ± standard deviation (SD). *P* < 0.05 was considered statistically significant.

## Results

### CIMT improves motor function in rats with cerebral ischemia

The foot-fault test was performed on days 7, 14, and 21 post

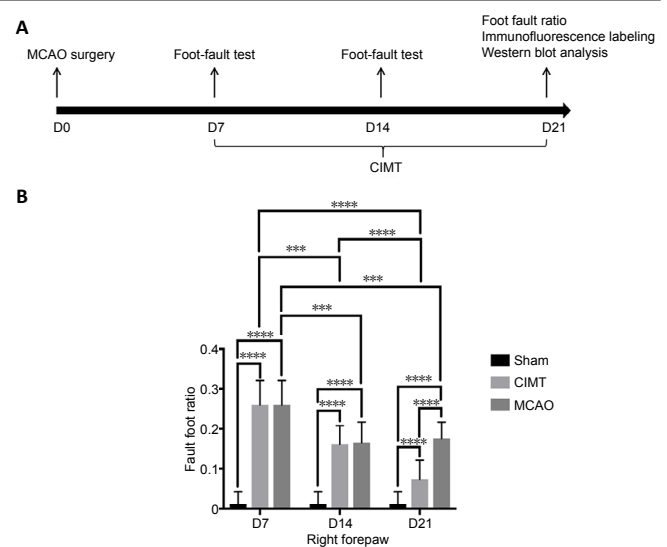


**Figure 1 | CIMT improves motor function in rats with cerebral ischemia.**

(A) Flow chart of the experimental design. (B) Foot fault ratio of the right forelimb. Data are expressed as the mean ± SD. \*\*\**P* < 0.001, \*\*\*\**P* < 0.0001 (two-way analysis of variance and Tukey's multiple comparisons test). CIMT: Constraint-induced movement therapy; MCAO: Middle cerebral artery occlusion.

stroke. At 7 days, foot fault ratios of the right forelimb were significantly higher in the CIMT and MCAO groups than in the sham group (*P* < 0.0001), with no significant difference between CIMT and MCAO groups (*P* > 0.9999). After 1 week of CIMT, an obvious deficit still existed in the CIMT group and there was no change in the MCAO group (*P* = 0.9838). However, after 2 weeks of CIMT, the foot fault ratio of the right forelimb was significantly lower in the CIMT group than in the MCAO group (*P* < 0.0001). Additionally, the ratio in the MCAO group was decreased on day 14 but not on day 21, while that in the CIMT group continued to decrease during these 2 weeks (Figure 1B). Thus, although rats in the CIMT group still showed right forelimb dysfunction compared to the sham group after 2 weeks of CIMT, these data indicate that 2 weeks of CIMT can improve motor function in rats following ischemic stroke.

### CIMT increases GluR2-containing synapses while reducing AMPARs lacking GluR2 in the ipsilateral sensorimotor cortex

In the ipsilateral sensorimotor cortex, colocalization of NR1 with GluR2 was higher (*P* < 0.0001; Figure 2A and B) whereas colocalization of NR1 with GluR1 was lower (*P* < 0.0001; Figure 2A and B) in the CIMT group than in the MCAO group. Thus, CIMT increased the number of GluR2-containing functional synapses while reducing the abundance of AMPARs lacking GluR2 in the ipsilateral sensorimotor cortex during the chronic phase of ischemic stroke.

### CIMT decreases the number of AMPARs lacking GluR2 in the ipsilateral hippocampus CA3 region

In the ipsilateral hippocampus CA1 region, colocalization of NR1 with GluR2 was higher in the MCAO group than in the other 2 groups (sham vs. MCAO, *P* = 0.0036; CIMT vs. MCAO, *P* = 0.0129; Figure 3A), whereas colocalization of NR1 with GluR1 was similar across groups (sham vs. CIMT, *P* = 0.9958; sham vs. MCAO, *P* = 0.0970; CIMT vs. MCAO, *P* = 0.1248; Figure 3B). These results indicate that AMPARs at functional synapses of the MCAO group are mainly GluR2/GluR3 heteromeric receptors. In the ipsilateral CA3 region, colocalization of NR1 with GluR1 was higher in the MCAO group than in the other two groups (sham vs. MCAO, *P* = 0.0017; CIMT vs. MCAO, *P* = 0.0340; Figure 3D). There was no significant difference in the colocalization of NR1 with GluR2 between groups (sham vs. CIMT, *P* = 0.9924; sham vs. MCAO, *P* = 0.8603; CIMT vs. MCAO, *P* = 0.7530; Figure 3C). Thus,

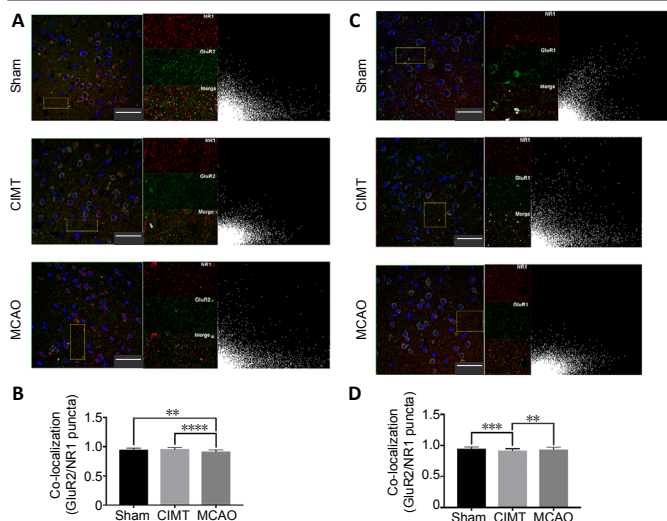


**Figure 2 | CIMT increases colocalization of NR1 with GluR2 while reducing that of NR1 with GluR1 in the ipsilateral sensorimotor cortex.**

(A) Confocal images of NR1 (red, Cy3) and GluR2 (green, Alexa Fluor 488) double-immunolabeling in the sensorimotor cortex. Selected areas other than neuronal nuclei (with DAPI staining) were used for colocalization analysis. The right image shows a scatterplot of the correlation between NR1 and GluR2 distributions; x and y axes show values for the red and green fluorescence channels, respectively. Scale bars: 50  $\mu$ m. (B) Colocalization of NR1 with GluR2 was lower in the MCAO group than in the other two groups ( $P < 0.01$  or  $< 0.0001$ ). (C) Confocal images of NR1 (red, Cy3) and GluR1 (green, Alexa Fluor 488) double-immunolabeling in the sensorimotor cortex. Selected areas other than neuronal nuclei (stained with DAPI) were used for colocalization analysis. The right image shows a scatterplot of the correlation between NR1 and GluR1 distributions; x and y axes show values for the red and green fluorescence channels, respectively. Scale bars: 50  $\mu$ m. (D) Colocalization of NR1 with GluR1 was lower in the CIMT group than in the other two groups ( $P < 0.01$  or  $< 0.001$ ). Data are expressed as the mean  $\pm$  SD.  $**P < 0.01$ ,  $***P < 0.001$ ,  $****P < 0.0001$  (one-way analysis of variance followed by Tukey's multiple comparisons test). CIMT: Constraint-induced movement therapy; GluR: glutamate receptor; MCAO: middle cerebral artery occlusion.

CIMT abrogated the increase in AMPARs lacking GluR2 that was observed following stroke.

**CIMT increases total synaptic and surface AMPAR expression in the ipsilateral sensorimotor cortex and hippocampus**

In the ipsilateral sensorimotor cortex, total GluR1 and total GluR2 expression in synaptosomes was higher in the CIMT group than in the MCAO group (total GluR1:  $P = 0.0088$ ; total GluR2:  $P = 0.0384$ ; **Figure 4A-a, b**). Moreover, compared to the MCAO group, surface GluR1 expression was elevated in the CIMT group ( $P = 0.0420$ , **Figure 4A-c**). In contrast, surface GluR2 levels did not differ between groups (sham vs. CIMT,  $P = 0.8253$ ; sham vs. MCAO,  $P = 0.8746$ ; CIMT vs. MCAO,  $P = 0.9893$ ; **Figure 4A-d**). In the ipsilateral hippocampus, surface GluR1 and GluR2 expression was higher in the CIMT group than in the MCAO group (surface GluR1:  $P = 0.0225$ ; surface GluR2:  $P = 0.0330$ ; **Figure 4B-c, d**). However, total GluR1 and GluR2 levels in the synaptosome protein fraction were similar across groups (total GluR1: sham vs. CIMT,  $P = 0.7622$ , sham vs. MCAO,  $P = 0.4107$ , CIMT vs. MCAO,  $P = 0.1261$ ; total GluR2: sham vs. CIMT,  $P = 0.9487$ ; sham vs. MCAO,  $P = 0.6705$ , CIMT vs. MCAO,  $P = 0.8193$ ; **Figure 4B-a, b**). These data indicate that CIMT not only increases the expression of synaptic AMPARs but also that of AMPARs on the synaptic membrane in ipsilateral brain areas. Representative results of the western blot analysis are shown in **Figure 4C**.

**Discussion**

CIMT involves the forced use of the impaired limb while restricting that of the contralateral limb in daily activities. This method is widely used in post-stroke rehabilitation to improve

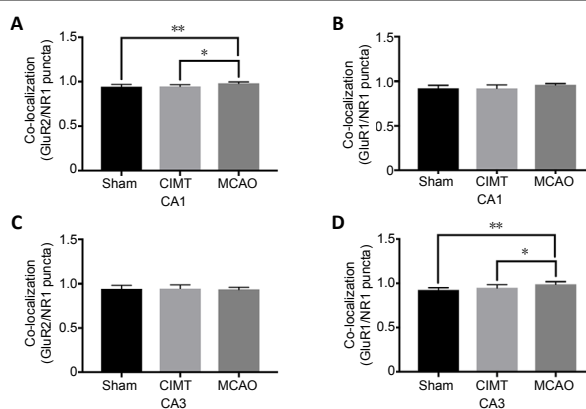


**Figure 3 | Effect of CIMT on the colocalization of NR1 with GluR1/GluR2 in the ipsilateral hippocampus.**

(A, C) Colocalization of NR1 with GluR2 in the CA1 (A) and CA3 (C) areas of the ipsilateral hippocampus. (B, D) Colocalization of NR1 with GluR1 in the CA1 (B) and CA3 (D) areas of the ipsilateral hippocampus. Confocal images of NR1 (red) and GluR2 (green) and of NR1 (red) and GluR1 (green) double-immunolabeling in the hippocampus are shown in Additional Figures 1–4. Data are expressed as the mean  $\pm$  SD.  $*P < 0.05$ ,  $**P < 0.01$  (one-way analysis of variance followed by Tukey's multiple comparisons test). CIMT: Constraint-induced movement therapy; GluR: glutamate receptor; MCAO: middle cerebral artery occlusion.

the motor function of impaired upper limbs (Zhao et al., 2009; Kwakkel et al., 2015; Qu et al., 2015). Accordingly, in the present study as well as our previous work, we found that CIMT improved motor function in rats with ischemic stroke (Hu et al., 2019; Liu et al., 2019). The mechanisms underlying the effects of CIMT may be related to functional reorganization and structural plasticity in the brain (Yoon et al., 2014; Qu et al., 2015). It was previously reported that CIMT promoted post-stroke synaptic plasticity and improved behavioral outcome by inducing the formation of synapses and enhancing synaptophysin and postsynaptic density-95 expression (Zhao et al., 2009, 2013). Activity-dependent AMPAR trafficking has been well-studied in the context of synaptic plasticity and remodeling (Henley, 2003; Sheng and Hyung Lee, 2003). The distribution of AMPARs in the postsynaptic membrane is tightly regulated through lateral diffusion, endocytosis, and exocytosis (Lussier et al., 2012). We therefore measured the surface expression of AMPARs in the present study and found that CIMT enhanced AMPAR-dependent synaptic plasticity in the ipsilateral sensorimotor cortex and hippocampus following stroke.

CIMT increased the colocalization of NR1 with GluR2 while decreasing that of NR1 with GluR1 in the ipsilateral sensorimotor cortex. These data suggest that CIMT increased GluR2-containing functional synapses. There are two possible explanations for these results. GluR2-positive synapses in the CIMT group mostly comprised GluR2/3 heteromers rather than GluR1/2 heteromers. Alternatively, it is possible that more AMPARs lacking GluR2 existed in the MCAO group. The latter is the more likely explanation because GluR2/3 heteromers are rare in the cortex and hippocampus. Our results are consistent with the GluR2 hypothesis following stroke, which suggests that delayed neuronal death following cerebral ischemia could be due to reduced surface expression of GluR2 and upregulation of AMPARs lacking GluR2, resulting in an abnormal increase in calcium influx (Pellegrini-Giampietro et al., 1997; Wang et al., 2011) given that the latter are calcium-permeable and exhibit a high single-channel conductance (Bowie and Mayer, 1995; Geiger et al., 1995). Inhibiting GluR2 internalization or the decreases in GluR2 mRNA and protein levels after ischemic injury is thought to have neuroprotective effects (Dixon et al., 2009; Montori et al., 2010; Wang et al., 2011; Zhai et al., 2013; Chen et al., 2014). Another study found that redistribution of GluR1 receptors on the synaptic membrane surface enhanced neuronal death following oxygen glucose deprivation; conversely, preventing the oxygen

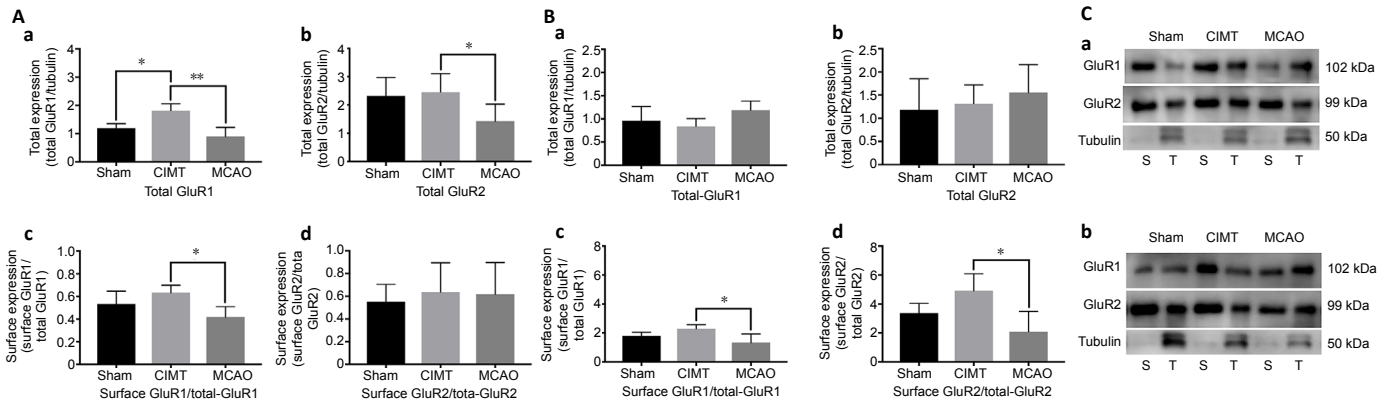


**Figure 4 | CIMT increases total synaptic and surface AMPAR expression in the ipsilateral hemisphere.**

(A) In the ipsilateral sensorimotor cortex, total synaptic GluR1 and GluR2 (a, b) and surface GluR1 (c) expression was higher in the CIMT group than in the MCAO group; surface expression of GluR2 was increased in the CIMT group, but this was non-significant (d). (B) In the ipsilateral hippocampus, total synaptic GluR1 and GluR2 levels did not differ between groups (a, b). However, surface GluR1 and GluR2 levels were higher in the CIMT group than

in the MCAO group (c, d). (C) Tubulin, which is not present in the membrane fraction, served as a reference to test the purity of the extracted membrane proteins. Data are expressed as the mean  $\pm$  SD. \* $P < 0.05$ , \*\* $P < 0.01$  (one-way analysis of variance followed by Tukey's multiple comparisons test). AMPAR:  $\alpha$ -Amino-3-hydroxy-5-methyl-4-isoxazole propionic acid receptor; CIMT: constraint-induced movement therapy; GluR: glutamate receptor; MCAO: middle cerebral artery occlusion; S: membrane surface protein; T: synaptic total protein.

glucose deprivation-induced increase in GluR1 membrane insertion alleviated neuronal death (Al Rahim and Hossain, 2013). One study found that blocking GluR2 internalization had long-term neuroprotective effects that persisted for 28 days after MCAO. Accordingly, we speculate that CIMT increases the number of GluR2-containing functional synapses and decreases the number of AMPARs lacking GluR2 in the ipsilateral sensorimotor cortex during the chronic phase of stroke, thereby contributing to behavioral improvement.

Finally, we did not examine the expression of GluR3, which could better corroborate our findings.

AMPA abundance and dynamics on the postsynaptic membrane influence synaptic strength and plasticity (Bredt and Nicoll, 2003; Huganir and Nicoll, 2013). AMPAR-mediated synaptic transmission can be enhanced by increasing the number of AMPARs at a single synapse or the number of functional synapses (Arendt et al., 2013; Ba et al., 2016). In this study we observed functional changes that were associated with alterations in AMPAR surface expression. We found that CIMT not only enhanced total synaptic GluR1 and GluR2 levels but also surface GluR1 expression, which was abrogated by the decrease in GluR1-containing AMPARs in the CIMT group observed by immunofluorescence analysis. Total GluR2 expression was much higher than total GluR1 and the same trend was observed for surface expression, indicating that the increased surface levels of GluR1 did not reflect an increase in AMPARs lacking GluR2. In the ipsilateral hippocampus, CIMT enhanced surface expression of GluR1 while total GluR2 level was unchanged. Previous studies have shown that GluR1 and GluR2 mRNA levels and surface localization were reduced in many brain areas including the cerebral cortex and hippocampus in rats following cerebral ischemia (Montori et al., 2010; Chen et al., 2014). Various motor exercises increased GluR1 and GluR2 expression after ischemic stroke (Real et al., 2010; Clarkson et al., 2011; Kintz et al., 2013), which is consistent with our findings. Furthermore, we showed that CIMT increased surface GluR1 and GluR2 expression in ipsilateral brain areas.

In conclusion, CIMT not only increased the number of GluR2-containing functional synapses in the ipsilateral sensorimotor cortex, but also decreased the abundance of AMPARs lacking GluR2 in the ipsilateral sensorimotor cortex and hippocampal CA3 region. It also enhanced the expression of synaptic AMPARs in the ipsilateral sensorimotor cortex and surface expression of synaptic AMPARs in the ipsilateral sensorimotor cortex and hippocampus. Thus, CIMT improves motor function following ischemic stroke by strengthening synaptic transmission in the sensorimotor cortex and hippocampus, highlighting its clinical value for restoring limb movement in stroke patients.

Our study had some shortcomings. Firstly, we quantified functional synapses and surface GluR1 and GluR2 expression by immunofluorescence labeling and biotinylation. However, electrophysiology is a more accurate way to assess synaptic transmission. Changes in the abundance of AMPARs lacking GluR2 can be observed by measuring the rectification index of AMPAR excitatory postsynaptic potentials. Therefore, the results of the present study must be validated using electrophysiology. Secondly, we did not measure changes in functional synapses and AMPAR abundance and subunit composition in the acute phase after cerebral ischemia.

**Author contributions:** Study concept and design: YLB, CC, JH; data collection: JH, PLL, YYW; data analysis: YH, BYG; statistical analysis and manuscript preparation: JH, PLL, YH; manuscript editing and review: YLB, CC, YYW. All authors approved the final version of the manuscript.

**Conflicts of interest:** The authors declare that they have no competing interests.

**Financial support:** This study was supported by the National Natural Science Foundation of China, Nos. 81871841 (to YLB) and 81601960 (to CC). The funders had no roles in the study design, conduction of experiment, data collection and analysis, decision to publish, or preparation of the manuscript.

**Institutional review board statement:** All experimental procedures and protocols were approved by the Department of Laboratory Animal Science of Fudan University, China (approval No. 201802173S) on March 3, 2018. All experimental procedures described here were in accordance with the National Institutes of Health (NIH) Guidelines for the Care and Use of Laboratory Animals (NIH Publication No. 85-23, revised 1996).

**Copyright license agreement:** The Copyright License Agreement has been signed by all authors before publication.

**Data sharing statement:** Datasets analyzed during the current study are available from the corresponding author on reasonable request.

**Plagiarism check:** Checked twice by iThenticate.

**Peer review:** Externally peer reviewed.

**Open access statement:** This is an open access journal, and articles are distributed under the terms of the Creative Commons Attribution-NonCommercial-ShareAlike 4.0 License, which allows others to remix, tweak, and build upon the work non-commercially, as long as appropriate credit is given and the new creations are licensed under the identical terms.

**Additional files:**

**Additional Figure 1:** Effect of CIMT on the colocalization of NR1 with GluR2 in ipsilateral hippocampal CA1 region (double immunofluorescence staining).

**Additional Figure 2:** Effect of CIMT on the colocalization of NR1 with

*GluR1 in ipsilateral hippocampal CA1 region (double immunofluorescence staining).*

**Additional Figure 3:** *Effect of CIMT on the colocalization of NR1 with GluR2 in ipsilateral hippocampal CA3 region (double immunofluorescence staining).*

**Additional Figure 4:** *Effect of CIMT on the colocalization of NR1 with GluR1 in ipsilateral hippocampal CA3 region (double immunofluorescence staining).*

## References

Al Rahim M, Hossain MA (2013) Genetic deletion of NP1 prevents hypoxic-ischemic neuronal death via reducing AMPA receptor synaptic localization in hippocampal neurons. *J Am Heart Assoc* 2:e006098.

Alia C, Spalletti C, Lai S, Panarese A, Lamola G, Bertolucci F, Vallone F, Di Garbo A, Chisari C, Micera S, Caleo M (2017) Neuroplastic changes following brain ischemia and their contribution to stroke recovery: novel approaches in neurorehabilitation. *Front Cell Neurosci* 11:76.

Anggono V, Huganir RL (2012) Regulation of AMPA receptor trafficking and synaptic plasticity. *Curr Opin Neurobiol* 22:461-469.

Arendt KL, Sarti F, Chen L (2013) Chronic inactivation of a neural circuit enhances LTP by inducing silent synapse formation. *J Neurosci* 33:2087-2096.

Arya KN, Pandian S, Verma R, Garg RK (2011) Movement therapy induced neural reorganization and motor recovery in stroke: a review. *J Bodyw Mov Ther* 15:528-537.

Askim T, Indredavik B, Håberg A (2010) Internally and externally paced finger movements differ in reorganization after acute ischemic stroke. *Arch Phys Med Rehabil* 91:1529-1536.

Askim T, Indredavik B, Vangberg T, Håberg A (2009) Motor network changes associated with successful motor skill relearning after acute ischemic stroke: a longitudinal functional magnetic resonance imaging study. *Neurorehabil Neural Repair* 23:295-304.

Ba W, Seltén MM, van der Raadt J, van Veen H, Li LL, Benevento M, Oudakker AR, Lasabuda RSE, Letteboer SJ, Roepman R, van Wezel RJA, Courtney MJ, van Bokhoven H, Nadif Kasri N (2016) ARHGAP12 functions as a developmental brake on excitatory synapse function. *Cell Rep* 14:1355-1368.

Benjamin EJ, Virani SS, Callaway CW, Chamberlain AM, Chang AR, Cheng S, Chiuve SE, Cushman M, Delling FN, Deo R, de Ferranti SD, Ferguson JF, Fornage M, Gillespie C, Isasi CR, Jiménez MC, Jordan LC, Judd SE, Lackland D, Lichtman JH, et al. (2018) Heart Disease and Stroke Statistics-2018 update: a report from the American Heart Association. *Circulation* 137:e67-e492.

Bowie D, Mayer ML (1995) Inward rectification of both AMPA and kainate subtype glutamate receptors generated by polyamine-mediated ion channel block. *Neuron* 15:453-462.

Bredt DS, Nicoll RA (2003) AMPA receptor trafficking at excitatory synapses. *Neuron* 40:361-379.

Bueteftsch CM (2015) Role of the contralateral hemisphere in post-stroke recovery of upper extremity motor function. *Front Neurol* 6:214.

Carmichael ST (2012) Brain excitability in stroke: the yin and yang of stroke progression. *Arch Neurol* 69:161-167.

Carroll RC, Beattie EC, von Zastrow M, Malenka RC (2001) Role of AMPA receptor endocytosis in synaptic plasticity. *Nat Rev Neurosci* 2:315-324.

Chen Z, Xiong C, Pancyr C, Stockwell J, Walz W, Cayabyab FS (2014) Prolonged adenosine A1 receptor activation in hypoxia and pial vessel disruption focal cortical ischemia facilitates clathrin-mediated AMPA receptor endocytosis and long-lasting synaptic inhibition in rat hippocampal CA3-CA1 synapses: differential regulation of GluA2 and GluA1 subunits by p38 MAPK and JNK. *J Neurosci* 34:9621-9643.

Clarkson AN, Overman JJ, Zhong S, Mueller R, Lynch G, Carmichael ST (2011) AMPA receptor-induced local brain-derived neurotrophic factor signaling mediates motor recovery after stroke. *J Neurosci* 31:3766-3775.

Cull-Candy S, Kelly L, Farrant M (2006) Regulation of Ca<sup>2+</sup>-permeable AMPA receptors: synaptic plasticity and beyond. *Curr Opin Neurobiol* 16:288-297.

Dixon RM, Mellor JR, Hanley JG (2009) PICK1-mediated glutamate receptor subunit 2 (GluR2) trafficking contributes to cell death in oxygen/glucose-deprived hippocampal neurons. *J Biol Chem* 284:14230-14235.

Gao BY, Xu DS, Liu PL, Li C, Du L, Hua Y, Hu J, Hou JY, Bai YL (2020) Modified constraint-induced movement therapy alters synaptic plasticity of rat contralateral hippocampus following middle cerebral artery occlusion. *Neural Regen Res* 15:1045-1057.

Geiger JR, Melcher T, Koh DS, Sakmann B, Seeburg PH, Jonas P, Monyer H (1995) Relative abundance of subunit mRNAs determines gating and Ca<sup>2+</sup> permeability of AMPA receptors in principal neurons and interneurons in rat CNS. *Neuron* 15:193-204.

Greger IH, Khatri L, Ziff EB (2002) RNA editing at arg607 controls AMPA receptor exit from the endoplasmic reticulum. *Neuron* 34:759-772.

Henley JM (2003) Protein interactions implicated in AMPA receptor trafficking: a clear destination and an improving route map. *Neurosci Res* 45:243-254.

Hofmeijer J, Mulder AT, Farinha AC, van Putten MJ, le Feber J (2014) Mild hypoxia affects synaptic connectivity in cultured neuronal networks. *Brain Res* 1557:180-189.

Hu J, Li C, Hua Y, Zhang B, Gao BY, Liu PL, Sun LM, Lu RR, Wang YY, Bai YL (2019) Constraint-induced movement therapy promotes motor function recovery by enhancing the remodeling of ipsilesional corticospinal tract in rats after stroke. *Brain Res* 1708:27-35.

Hua Y, Li C, Hu J, Wang YY, Liu PL, Gao BY, Chen C, Xu DS, Zhang B, Bai YL (2019) Fluoxetine adjunct to therapeutic exercise promotes motor recovery in rats with cerebral ischemia: Roles of nucleus accumbens. *Brain Res Bull* 153:1-7.

Huganir RL, Nicoll RA (2013) AMPARs and synaptic plasticity: the last 25 years. *Neuron* 80:704-717.

Isaac JT, Ashby MC, McBain CJ (2007) The role of the GluR2 subunit in AMPA receptor function and synaptic plasticity. *Neuron* 54:859-871.

Jones TA, Adkins DL (2015) Motor system reorganization after stroke: stimulating and training toward perfection. *Physiology (Bethesda)* 30:358-370.

Kintz N, Petzinger GM, Akopian G, Ptasnik S, Williams C, Jakowec MW, Walsh JP (2013) Exercise modifies  $\alpha$ -amino-3-hydroxy-5-methyl-4-isoxazolepropionic acid receptor expression in striatopallidal neurons in the 1-methyl-4-phenyl-1,2,3,6-tetrahydropyridine-lesioned mouse. *J Neurosci Res* 91:1492-1507.

Kwakkel G, Veerbeek JM, van Wegen EE, Wolf SL (2015) Constraint-induced movement therapy after stroke. *Lancet Neurol* 14:224-234.

Li W, Huang R, Shetty RA, Thangthaeng N, Liu R, Chen Z, Sumien N, Rutledge M, Dillon GH, Yuan F, Forster MJ, Simpkins JW, Yang SH (2013) Transient focal cerebral ischemia induces long-term cognitive function deficit in an experimental ischemic stroke model. *Neurobiol Dis* 59:18-25.

Liu P, Li C, Zhang B, Zhang Z, Gao B, Liu Y, Wang Y, Hua Y, Hu J, Qiu X, Bai Y (2019) Constraint induced movement therapy promotes contralesional-oriented structural and bihemispheric functional neuroplasticity after stroke. *Brain Res Bull* 150:201-206.

Lu W, Shi Y, Jackson AC, Bjorgan K, Doring MJ, Sprengel R, Seeburg PH, Nicoll RA (2009) Subunit composition of synaptic AMPA receptors revealed by a single-cell genetic approach. *Neuron* 62:254-268.

Lussier MP, Herring BE, Nasu-Nishimura Y, Neutzner A, Karbowski M, Youle RJ, Nicoll RA, Roche KW (2012) Ubiquitin ligase RNF167 regulates AMPA receptor-mediated synaptic transmission. *Proc Natl Acad Sci U S A* 109:19426-19431.

Malinow R, Malenka RC (2002) AMPA receptor trafficking and synaptic plasticity. *Annu Rev Neurosci* 25:103-126.

Mokin M, Keifer J (2006) Quantitative analysis of immunofluorescent punctate staining of synaptically localized proteins using confocal microscopy and stereology. *J Neurosci Methods* 157:218-224.

Montori S, Dos Anjos S, Ríos-Granja MA, Pérez-García CC, Fernández-López A, Martínez-Villayandre B (2010) AMPA receptor downregulation induced by ischaemia/reperfusion is attenuated by age and blocked by meloxicam. *Neuropathol Appl Neurobiol* 36:436-447.

Nie J, Yang X (2017) Modulation of synaptic plasticity by exercise training as a basis for ischemic stroke rehabilitation. *Cell Mol Neurobiol* 37:5-16.

Park HA, Licznernski P, Alavian KN, Shanabrough M, Jonas EA (2015) Bcl-xL is necessary for neurite outgrowth in hippocampal neurons. *Antioxid Redox Signal* 22:93-108.

Pellegrini-Giampietro DE, Gorter JA, Bennett MV, Zukin RS (1997) The GluR2 (GluR-B) hypothesis: Ca<sup>2+</sup>-permeable AMPA receptors in neurological disorders. *Trends Neurosci* 20:464-470.

Qu HL, Zhao M, Zhao SS, Xiao T, Song CG, Cao YP, Jolkkonen J, Zhao CS (2015) Forced limb-use enhanced neurogenesis and behavioral recovery after stroke in the aged rats. *Neuroscience* 286:316-324.

Real CC, Ferreira AF, Hernandez MS, Britto LR, Pires RS (2010) Exercise-induced plasticity of AMPA-type glutamate receptor subunits in the rat brain. *Brain Res* 1363:63-71.

Sheng M, Hyoung Lee S (2003) AMPA receptor trafficking and synaptic plasticity: major unanswered questions. *Neurosci Res* 46:127-134.

Shimshak DR, Jensen V, Celikel T, Geng Y, Schupp B, Bus T, Mack V, Marx V, Hvalby Ø, Seeburg PH, Sprengel R (2006) Forebrain-specific glutamate receptor B deletion impairs spatial memory but not hippocampal field long-term potentiation. *J Neurosci* 26:8428-8440.

Wang H, Luo M, Li C, Wang G (2011) Propofol post-conditioning induced long-term neuroprotection and reduced internalization of AMPAR GluR2 subunit in a rat model of focal cerebral ischemia/reperfusion. *J Neurochem* 119:210-219.

Wang L, Yu C, Chen H, Qin W, He Y, Fan F, Zhang Y, Wang M, Li K, Zang Y, Woodward TS, Zhu C (2010) Dynamic functional reorganization of the motor execution network after stroke. *Brain* 133:1224-1238.

Wang M, Li S, Zhang H, Pei L, Zou S, Lee FJ, Wang YT, Liu F (2012) Direct interaction between GluR2 and GAPDH regulates AMPAR-mediated excitotoxicity. *Mol Brain* 5:13.

Wenthold RJ, Petralia RS, Blahos J, II, Niedzielski AS (1996) Evidence for multiple AMPA receptor complexes in hippocampal CA1/CA2 neurons. *J Neurosci* 16:1982-1989.

Writing Group Members, Mozaffarian D, Benjamin EJ, Go AS, Arnett DK, Blaha MJ, Cushman M, Das SR, de Ferranti S, Després JP, Fullerton HJ, Howard VJ, Huffman MD, Isasi CR, Jiménez MC, Judd SE, Kissela BM, Lichtman JH, Lisabeth LD, Liu S, et al. (2016) Heart Disease and Stroke Statistics-2016 Update: A Report From the American Heart Association. *Circulation* 133:e38-360.

Xie Q, Cheng J, Pan G, Wu S, Hu Q, Jiang H, Wang Y, Xiong J, Pang Q, Chen X (2019) Treadmill exercise ameliorates focal cerebral ischemia/reperfusion-induced neurological deficit by promoting dendritic modification and synaptic plasticity via upregulating caveolin-1/VEGF signaling pathways. *Exp Neurol* 313:60-78.

Yoon JA, Koo BI, Shin MJ, Shin YB, Ko HY, Shin YI (2014) Effect of constraint-induced movement therapy and mirror therapy for patients with subacute stroke. *Ann Rehabil Med* 38:458-466.

Zhai D, Li S, Wang M, Chin K, Liu F (2013) Disruption of the GluR2/GAPDH complex protects against ischemia-induced neuronal damage. *Neurobiol Dis* 54:392-403.

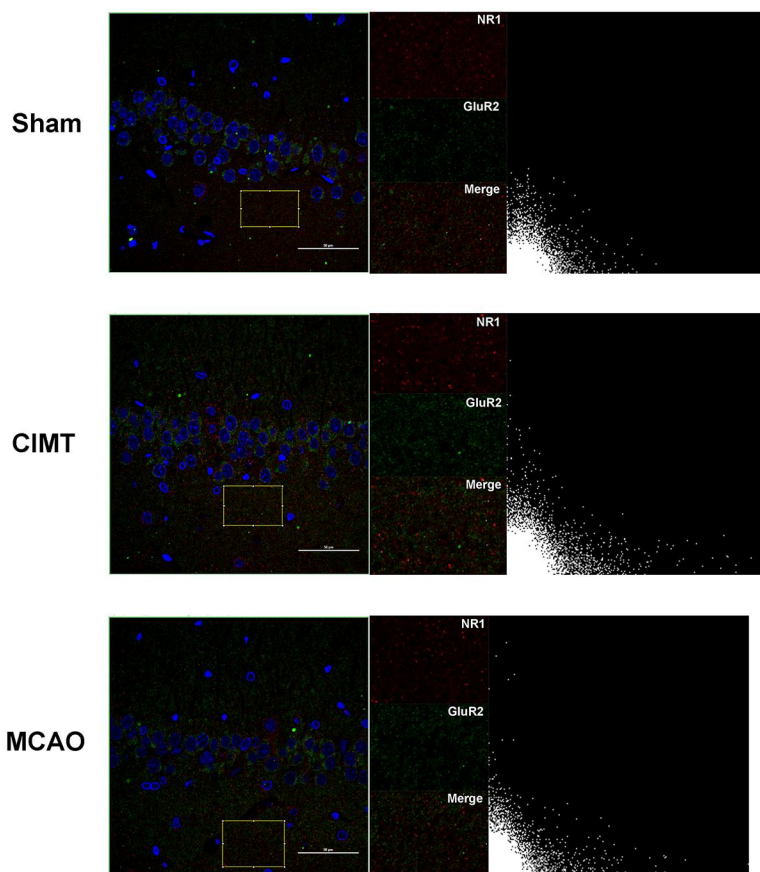
Zhao C, Wang J, Zhao S, Nie Y (2009) Constraint-induced movement therapy enhanced neurogenesis and behavioral recovery after stroke in adult rats. *Tohoku J Exp Med* 218:301-308.

Zhao SS, Zhao Y, Xiao T, Zhao M, Jolkkonen J, Zhao CS (2013) Increased neurogenesis contributes to the promoted behavioral recovery by constraint-induced movement therapy after stroke in adult rats. *CNS Neurosci Ther* 19:194-196.

Zhou C, Lippman JJ, Sun H, Jensen FE (2011) Hypoxia-induced neonatal seizures diminish silent synapses and long-term potentiation in hippocampal CA1 neurons. *J Neurosci* 31:18211-18222.

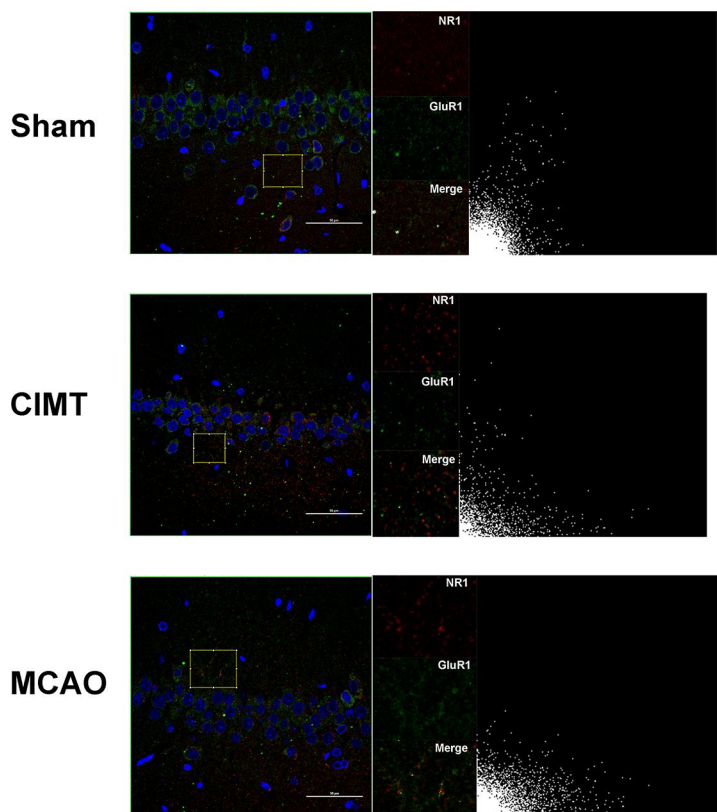
Zinchuk V, Zinchuk O, Okada T (2007) Quantitative colocalization analysis of multicolor confocal immunofluorescence microscopy images: pushing pixels to explore biological phenomena. *Acta Histochem Cytochem* 40:101-111.

C-Editor: Zhao M; S-Editors: Yu J, Li CH; L-Editors: Yu J, Song LP; T-Editor: Jia Y



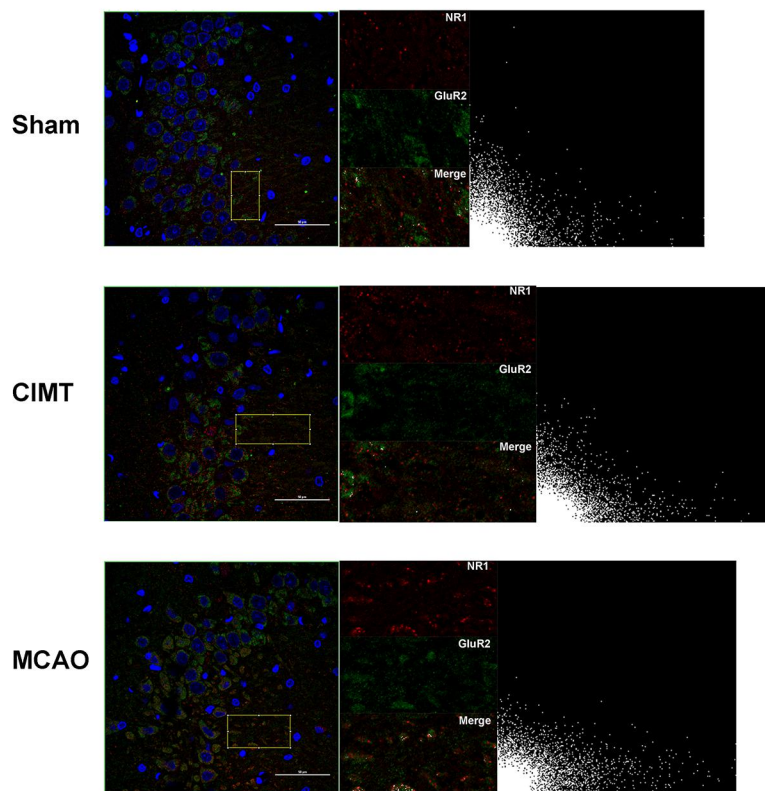
**Additional Figure 1 Effect of CIMT on the colocalization of NR1 with GluR2 in ipsilateral hippocampal CA1 region (double immunofluorescence staining).**

Double-immunolabeled confocal images for NR1 (red, stained by Cy3) and GluR2 (green, stained by Alexa Fluor 488) in CA1 area. Selecting areas other than neuron nuclei (with DAPI staining) were for colocalization analysis. The right image is a scatter plot of the correlation between NR1 and GluR2 distributions. The x-axis is the red fluorescence channel and the y-axis is the green fluorescence channel. The colocalization of NR1 with GluR2 in MCAO group was significantly higher than that in other two groups. Scale bars: 50 μm. CIMT: Constraint-induced movement therapy; DAPI: 4',6-diamidino-2-phenylindole; GluR2: glutamate receptor 2; MCAO: middle cerebral artery occlusion; NR1: glutamate receptor N-methyl-D-aspartic acid receptor 1.



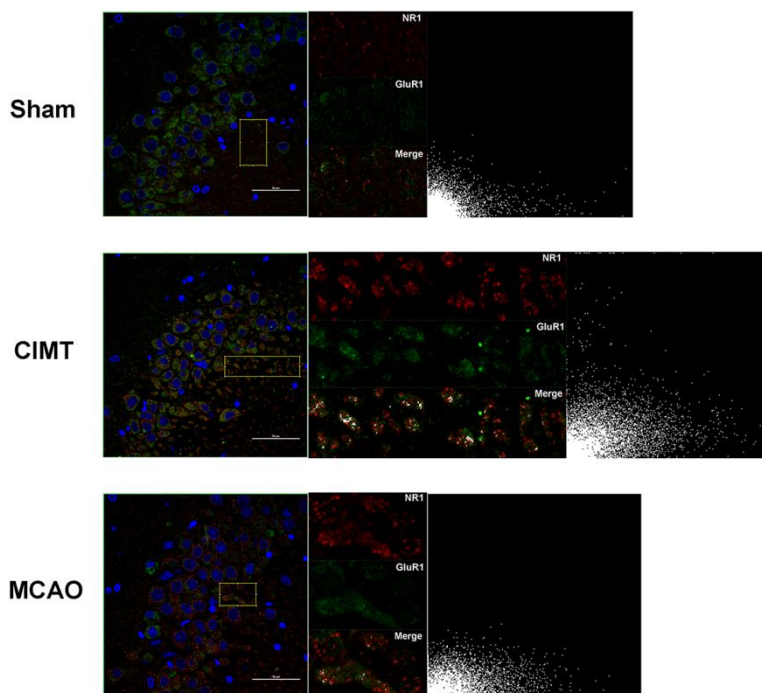
**Additional Figure 2 Effect of CIMT on the colocalization of NR1 with GluR1 in ipsilateral hippocampal CA1 region (double immunofluorescence staining).**

Double-immunolabeled confocal images for NR1 (red, stained by Cy3) and GluR1 (green, stained by Alexa Fluor 488) in CA1 area. Selecting areas other than neuron nuclei (with DAPI staining) were for colocalization analysis. The right image is a scatter plot of the correlation between NR1 and GluR1 distributions. The x-axis is the red fluorescence channel and the y-axis is the green fluorescence channel. There was no significant difference in colocalization of NR1 with GluR1 between groups. Scale bars: 50  $\mu$ m. CIMT: Constraint-induced movement therapy; DAPI: 4',6-diamidino-2-phenylindole; GluR1: glutamate receptor 1; MCAO: middle cerebral artery occlusion; NR1: glutamate receptor N-methyl-D-aspartic acid receptor 1.



**Additional Figure 3 Effect of CIMT on the colocalization of NR1 with GluR2 in ipsilateral hippocampal CA3 region (double immunofluorescence staining).**

Double-immunolabeled confocal images for NR1 (red, stained by Cy3) and GluR2 (green, stained by Alexa Fluor 488) in CA3 area. Selecting areas other than neuron nuclei (with DAPI staining) were for colocalization analysis. The right image is a scatter plot of the correlation between NR1 and GluR2 distributions. The x-axis is the red fluorescence channel and the y-axis is the green fluorescence channel. There was no significant difference in colocalization of NR1 with GluR2 between groups. Scale bars: 50  $\mu$ m. CIMT: Constraint-induced movement therapy; DAPI: 4',6-diamidino-2-phenylindole; GluR2: glutamate receptor 2; MCAO: middle cerebral artery occlusion; NR1: glutamate receptor N-methyl-D-aspartic acid receptor 1.



**Additional Figure 4 Effect of CIMT on the colocalization of NR1 with GluR1 in ipsilateral hippocampal CA3 region (double immunofluorescence staining).**

Double-immunolabeled confocal images for NR1 (red, stained by Cy3) and GluR1 (green, stained by Alexa Fluor 488) in CA3 area. Selecting areas other than neuron nuclei (with DAPI staining) were for colocalization analysis. The right image is a scatter plot of the correlation between NR1 and GluR1 distributions. The x-axis is the red fluorescence channel and the y-axis is the green fluorescence channel. The colocalization of NR1 with GluR1 in MCAO group was significantly higher than that in other two groups. Scale bars: 50  $\mu\text{m}$ . CIMT: Constraint-induced movement therapy; DAPI: 4',6-diamidino-2-phenylindole; GluR1: glutamate receptor 1; MCAO: middle cerebral artery occlusion; NR1: glutamate receptor N-methyl-D-aspartic acid receptor 1.